Conversion of italian depleted gas reservoirs. Part 1: preliminary assessment for CO2 geological sequestration

DX.DOI.ORG//10.19199/2025.174.1121-9041.015

Conversion of italian depleted gas reservoirs. Part 1: preliminary assessment for CO_2 geological sequestration

Christoforos Benetatos*
Giorgio Giglio*
Candido Pirri*,**
Alessandro Suriano*
Nicolo' Santi Vasile*
Francesca Verga*
Dario Viberti*

* Politecnico di Torino, Department of Environment, Land and Infrastructure Engineering (DIATI), Torino
** Italian Institute of Technology – CSFT, Torino

Corresponding author:
francesca.verga@polito.it

This paper examines the potential of Italian depleted gas reservoirs, particularly in the offshore Adriatic Sea region, for CO_2 geological sequestration. A pairing publication will explore the option of converting these reservoirs into hydrogen storage sites. The relevant field data were taken from publicly available sources and categorized into main scenarios. Sensitivity analyses were performed on a set of simplified yet representative cases, varying the reservoir depth and volume, as well as the size of the confining aquifer. A 3D geological (static) model was set up for each scenario: the structural trap was assumed to be an anticline, and the reservoir made of turbiditic deposits. The geological models served as the input for 3D coupled geochemical-fluid flow (dynamic) numerical models, used for the simulation of the conversion of depleted gas reservoirs into CO_2 storage facilities. The mineralogic composition of the reservoir rock and the chemical composition and pH of the formation water were taken from the literature. After reproducing the natural gas production phase, CO_2 injection was simulated. Storage capacity and injectivity of the reservoirs, as well as the CO_2 geochemical interactions over time, were assessed to identify the most promising reservoir characteristics. The storage safety issues, including the geomechanical response induced by underground CO_2 injection, were not addressed as they were beyond the scope of the work.

Keywords: *CO_2 geological sequestration, underground fluid storage, coupled reservoir simulation, trapping mechanisms, geochemical reactions.*

1. Introduction

Currently, the global production of greenhouse gases exceeds 50 billion tons per year and CO_2 represents more than 70% of the total emissions (European Commission & Joint Research Centre, 2024).

Carbon Capture and Storage (CCS) is recognized internationally as a key technology for mitigating global warming and climate change (Carbon Sequestration Leadership Forum, 2021). Underground storage of anthropogenic CO_2 consists in injecting and permanently sequestering the fluid in deep geological formations. Depleted gas and oil reservoirs and deep saline aquifers are the favorite candidates for safe geological storage of CO_2 (European Commission & Joint Research Centre, 2024). Although saline aquifers can offer very large storage volumes, the original formation pressure must be exceeded to displace the water initially saturating the pores of the rock to accommodate the injected fluid, and the ability of the reservoir to contain the injected CO_2 needs to be properly assessed. Conversely, a significant level of knowledge is already available for depleted hydrocarbon-bearing fields: information about the geological, structural and petrophysical characteristics is inherited from the exploration and hydrocarbon production phases. Uncertainties are reduced or mitigated with significant economic and technical benefits (Verga, 2018).

The first project for Carbon Capture and Sequestration (CCS) was first proposed in the 1970s, but little research was done until the early 1990s, when the idea gained credibility through the work of various research groups (Ma *et al.*, 2022). One of the first attempts at subsurface disposal of acid gas (more than 98% content of CO_2) took place in the Alberta Basin of Canada and the United States and provided useful experience for future operations. After these first attempts, geological storage of CO_2 has grown from a concept of limited interest to one that is quite widely regarded as a potentially important mitigation option for global warming and climate change (Benetatos *et al.*, 2021; Bocchini *et al.*, 2017; Rocca & Viberti, 2013). In 1996, Statoil and its partners initiated the world's first large-scale storage project at the Sleipner Gas Field in the North Sea, injecting 0.9 million tonnes of CO_2 annually into a depleted gas field (Furre *et al.*, 2017). Later, several oil companies became increasingly interested in geological storage, particularly in CCS in depleted gas fields (Afagwu

If there are references to colour figures in the text, the articles are available in open-access mode on the site www.geam-journal.org

and Weijermars, 2024; Hansen *et al.*, 2013; Ringrose *et al.*, 2013; Shi *et al.*, 2013; Tanase *et al.*, 2021; Trupp *et al.*, 2021). Examples of CCS projects include In Salah (Algeria), that stored almost 3.5 million tonnes of CO_2 from 2004 to 2011, Snøhvit (Norway), which is operational since 2008, Tomakomai (Japan), that injected almost 0.3 million tonnes of CO_2 from 2016 to 2019, Gorgon (Australia), which operates since 2019 and currently stores some 1.8 million tonnes of CO_2 per year and, recently, Ravenna (Italy), targeting the injection of 4 million tonnes of CO_2 per year within 2030.

The scientific literature on CO_2 storage is truly vast, with thousands of documents, including journal and conference research papers, reviews, books, guidelines, and technical reports having been published over decades. Many of these works contributed to identifying criteria for the initial selection of CO_2 storage locations and the main mechanisms responsible for trapping CO_2 in underground geological formations.

The geological formations, typically sandstones, selected for CO_2 storage must have the capacity to store an adequate volume of CO_2, the ability to accept the injected CO_2 at the rate that is supplied, grant fluid confinement due to the presence of a thick sealing layer (made of clays, claystones or mudstones) overlying the reservoir, and offer seismic stability (Suriano *et al.*, 2022). Thus, some basic characteristics should be met by a good candidate for CO_2 storage (Celia *et al.*, 2015; Chadwick & British Geological Survey, 2008; Working Group III of the Intergovernmental Panel on Climate Change, 2005). The key parameters for storage site evaluation are reservoir volume; pressure and temperature conditions to ensure the CO_2 will be in its dense (supercritical) phase; permeability and thickness of the formation (for injectivity); formation water chemical composition and pH, from which occurrence of geochemical processes are largely dependent; formation heterogeneity, responsible for uneven CO_2 distribution; entry pressure of the caprock (at which CO_2 starts penetrating in the sealing layer) and fracturing pressure; mineralogical composition of the reservoir rock, with special attention to the quantity of reactive minerals such as carbonates, feldspars and micas; potential presence of seismogenic faults; and, stress regime.

Based on these criteria, Italy is rich in depleted gas reservoirs that fulfill the requirements for CO_2 storage, especially in the offshore Adriatic Sea region (Carpignano *et al.*, 2023). This paper provides a screening of such reservoirs to identify the best candidates by investigating their storage capacity and injectivity, and the geochemical interaction of CO_2 with the reservoir rocks and fluids.

To this end, a set of representative scenarios was defined based on the characteristics of the Italian depleted fields. A 3D geological (static) model was set up for each of these representative scenarios. The geological models served as the input for the coupled geochemical and dynamic models, used for the simulation of the conversion of depleted gas reservoirs into CO_2 storage facilities. A lateral aquifer was also reproduced because the production mechanism observed in almost all the gas fields discovered in Italy is gas expansion combined with water drive. The mineralogic composition of the reservoir rock and the chemical composition and pH of the formation water were taken from the literature. After reproducing the primary gas production phase based on the historical gas recovery and a shut-in period of approximately 15 years to mimic the current abandoned status of most fields, CO_2 injection was simulated under the constraint that the original formation pressure should not be exceeded. The storage capacity and injectivity were evaluated for each scenario. Furthermore, the geochemical interactions of injected CO_2 with the rock and the formation water over time were simulated to assess the impact of the different trapping mechanisms.

2. Reservoir data

The data for the characterization of the Italian depleted gas reservoirs, which are mostly located offshore in the Adriatic region, were collected from public sources (e.g., UNMIG website-VIDEPI project) and include average depth, geological formation, geological age, environment/lithology, number of wells, start and end of production, cumulative gas production, caprock thickness, and average petrophysical properties (porosity and absolute permeability). Based on the cumulative gas production and assuming a recovery factor ranging between 60% and 85%, depending on the prevailing production mechanism, the volume of the original gas in place was estimated.

The distributions of the reservoir data were analyzed to define three main classes, corresponding to the

Tab. 1 – Reservoir data for parametric analyses.

Parameter	Depth (m ss)	GOIP ($10^9 \cdot sm^3$)	Aquifer size (r_{aq}/r_{res})
Min	1000	1	1.5
Average	2000	5	5
Max	3000	10	10

minimum, average and maximum values of each key parameter: reservoir depth, volume of gas originally in place (GOIP) and aquifer size. The reservoir classes and the values of the key parameters are provided in Table 1.

In sedimentary basins with an average thermal gradient, storage is recommended in formations that lie at depths of 800 meters or deeper. Thus, depths shallower than 1000 m were excluded from the analyses as they are incompatible with the storage of CO_2 in supercritical conditions and, more generally, with the underground storage of fluids in safe conditions due to the relatively limited distance of the formation from the surface. Depths greater than 3000 m were also excluded, mainly due to the increased costs of managing deep storage systems.

The reservoir volume was associated with the GOIP. However, it should be noted that, due to the reservoir depletion, water invades the gas-bearing zone during primary production (and any subsequent field closure period) in the case of an active aquifer. Thus, the residual porous volume available for CO_2 sequestration without exceeding the initial formation pressure to displace the advancing aquifer can be significantly less than the volume originally occupied by natural gas.

In agreement with the majority of the Italian depleted reservoirs, the structural trap was assumed to be an anticline and the reservoir made of turbiditic deposits (alternations of sand, silt, clay) and having petrophysical properties consistent with those reported for the real fields. Furthermore, the decision was made to focus the geological modeling on a single gas-bearing level because thin layers are not suitable for commercial storage projects. Discontinuities such as faults or pinch-outs were not considered in this work to as the main target was to investigate the impact of the reservoir characteristics most relevant to CO_2 geological storage.

Lateral aquifers confining the reservoirs were also taken into account because the production mechanism observed in almost all the gas fields discovered in Italy is gas expansion combined with water drive. Aquifers with varying extensions were considered with their dimensions expressed according to the Carter-Tracy model (later used for water influx calculations), i.e., by the ratio between the aquifer outer radius, r_{aq}, and the reservoir outer radius, r_{res}. The dimensions of the aquifer reproduce a weak water drive (r_{aq}/r_{res} = 1.5), an intermediate water drive (r_{aq}/r_{res} = 5) and a strong aquifer (r_{aq}/r_{res} = 10), respectively.

3. Reservoir Models

Based on the parameters reported in Table 1 and the considerations previously made, reference 3D static models representative of the real reservoirs were generated.

All the models have the same dimensions, equal to 6100 × 6100 × 100 m^3, and are subdivided into 61 × 61 × 20 blocks (Fig. 1). Homogeneous petrophysical values were assigned to the reservoir (NTG = 80%, ϕ = 20%, S_{wi} = 30%). The natural gas originally saturating the reservoir is considered to be 100% methane.

Figure 1 shows a view of the 3D reservoir model with the adopted discretization into blocks (gridding) and the distribution of the initial gas saturation for the reservoir base case (model A).

The reference case (model A) was assigned intermediate characteristics, then sensitivities were made on the reservoir depth, GOIP and size of the confining aquifer. In models B, C, D, E, F and G, only one parameter was changed with respect to the reference scenario.

The minimum aquifer extension (r_{aq}/r_{res} = 1.5) was implemented as the base case because it represents the most common situation for the analyzed depleted gas reservoir.

A total of 7 different models were set up for the sensitivity analyses (Table 2).

The software GEM, by CMG, was

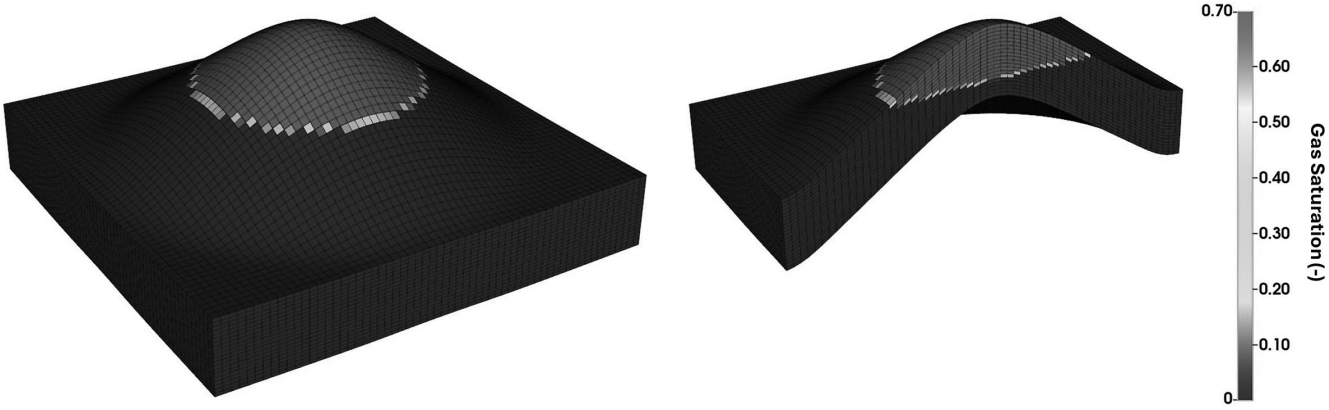

Fig. 1 – View of the 3D model with the adopted gridding and the distribution of the initial gas saturation for the reservoir base case (model A).

Tab. 2 – Model characteristics.

Model	Reservoir depth (m)	GOIP ($10^9 \cdot sm^3$)	Aquifer strength (r_{aq}/r_{res})
A (base case)	2000	5	1.5
B	1000	5	1.5
C	3000	5	1.5
D	2000	1	1.5
E	2000	10	1.5
F	2000	5	5
G	2000	5	10

used for performing the coupled geochemical-fluid flow simulations.

The PVT properties of the fluids (methane, CO_2, water) were calculated using the Peng-Robinson equation of state (Peng & Robinson, 1976), with the default parameters available in the software and provided in Table 3.

The water properties (compressibility, initial density and viscosity) are summarized in Table 4. The solubility of CO_2 in water was calculated through a modified version of Henry's law implemented in the software. The pH, salinity and chemical composition of the water, reported in Table 5, were taken from the real data publicly available for the Adriatic Sea fields (Table 5) (*ViDEPI*, s.d.).

The same absolute permeability (50 mD), anisotropy ratio (0.1), and gas-water relative permeability curves were adopted for all the models (fig. 2). The rock compressibility was set for each model according to the average reservoir depth.

The mineral composition of the reservoir rock assigned to all the models was taken from Spagnoli *et al.* (Spagnoli *et al.*, 2014) and is summarized in Table 6.

The initial pressure and temperature of the reservoir were defined based on the depth of the reservoir, adopting the hydrostatic gradient and an average thermal gradient, respectively.

The model characteristics and the values of the input parameters are summarized in Table 7.

Tab. 3 – Equations of state parameters.

Parameter	Methane	CO_2	Water
Molar weight (g/mol)	16.043	44.01	18.015
Acentric factor (-)	0.008	0.225	0.344
Critical pressure (atm)	45.4	72.8	217.6
Critical temperature (K)	190.6	304.2	647.3
Critical volume (m^3/kmol)	0.099	0.094	0.056
Parachor (-)	77	78	52
Specific Gravity (-)	0.3	0.818	1
Interaction coefficient to methane (-)	-	0.103	0.491
Interaction coefficient to water (-)	0.491	0.2	-

Tab. 4 – Water properties.

Water property	Model						
	A	B	C	D	E	F	G
Compressibility (kPa^{-1})	4e-7	3.8e-7	4.2e-7	4e-7	4e-7	4e-7	4e-7
Initial density SC (kg/m^3)	1021.7						
Viscosity (cP)	0.53	0.83	0.41	0.53	0.53	0.53	0.53

4. CO_2 trapping mechanisms

While consensus exists that CO_2 underground storage involves a number of different trapping mechanisms, the contribution of each one is challenging to assess as they

Tab. 5 – Water pH, salinity and chemical composition.

	Model	
	A, C, D, E, F, and G	B
pH	7.13	7.01
Equivalent salinity (g/l)	34.9	23.6
Equivalent salinity (mol/kg)	1.2	0.8
Na+ (ppm)	12409	8375
K+ (ppm)	177	63
Ca++ (ppm)	472	317
Mg+ (ppm)	554	538
Fe++ (ppm)	8	8
SiO_2 (ppm)	12	12
Cl- (ppm)	21173	14339

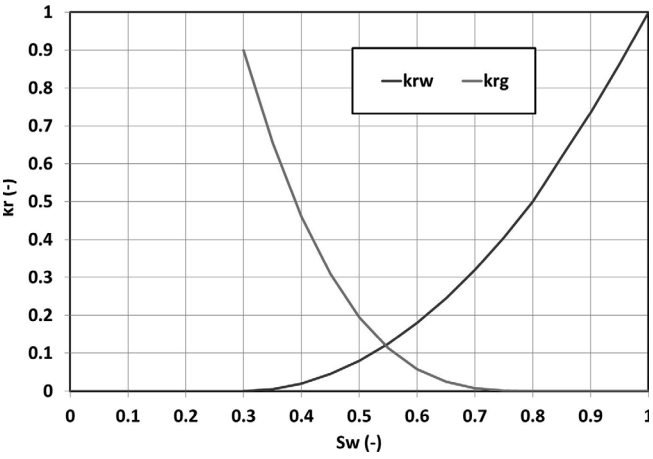

Fig. 2 – Relative permeability curves.

Tab. 6 – Reservoir rock mineral composition.

Mineral	Volume
Albite	4.2%
Anorthite	4.2%
Aragonite	7.1%
Calcite	26.3%
Chamosite	1.5%
Clinochlore	1.5%
Dolomite	0.1%
Halite	0.1%
Illite	0.1%
K-feldspar	6.2%
Kaolinite	0.1%
Muscovite	15.5%
Quartz	23%
Siderite	0.1%

Tab. 7 – Summary of the reservoir model characteristics and input data.

Parameter	Model						
	A	B	C	D	E	F	G
Reservoir							
Reference depth (m)	2000	1000	3000	2000	2000	2000	2000
Reference pressure (bar)	207.8	103.9	311.7	207.8	207.8	207.8	207.8
Reference temperature (°C)	64.9	32.5	97.4	64.9	64.9	64.9	64.9
Gas-Water Contact (m)	2076	1095	3069	2038	2101	2076	2076
Net-to-Gross (%)	80						
Porosity (%)	20						
Irreducible water saturation (%)	30						
Absolute permeability (mD)	50						
Anisotropy ratio (-)	0.1						
Rock compressibility (kPa^{-1})	2.6e-7	5.5e-7	1.7e-7	2.6e-7	2.6e-7	2.6e-7	2.6e-7
Carter-Tracy aquifer							
Thickness (m)	50						
Porosity (%)	20						
Absolute permeability (mD)	50						
r_{aq}/r_{res} (-)	1.5	1.5	1.5	1.5	1.5	5	10

largely depend on the fluid and rock properties of the reservoir as well as on the CO_2 injection strategy. Furthermore, the timescale associated with each of the sequestration mechanisms is very different. The mechanisms by which CO_2 can be trapped are:

1. structural/stratigraphic trapping is the confinement of the CO_2 by an impermeable cap rock. For pressure and temperature conditions above the critical point (p=74 bar and T= 31 °C), which correspond to a depth of approximately 1000 m, CO_2 is a supercritical fluid: while the CO_2 density is liquid-like, viscosity values remain gas-like. When CO_2 is injected into a depleted gas reservoir, a single miscible fluid phase consisting of natural gas and CO_2 is formed locally. However, although natural gas and CO_2 are fully miscible, instant mixing does not seem to occur in the reservoir and therefore, gravity segregation is an important issue.
2. residual or capillary trapping, which is the disconnection of the CO_2 phase into an immobile (trapped) fraction, is relevant in aquifers. In sedimentary rocks that do not contain organic material, including sandstones and carbonates, carbon dioxide is the non-wetting fluid relative to brine. As a result, during the injection stage, CO_2 displaces the aquifer (drainage process). However, after injection, the buoyant CO_2 migrates laterally and upward, and water displaces CO_2 in an imbibition-like process. This leads to the disconnection of the once-continuous plume and to the formation of residual gas (trapped CO_2). Water-CO_2 relative permeability hysteresis is a key factor in CO_2 residual trapping.
3. solubility trapping ($CO_2 + H_2O \leftrightarrow H_2CO_3$) describes the dissolution and hydration of CO_2 in the brine to form carbonic acid, possibly enhanced by gravity instabilities due to the larger density of the brine – CO_2 liquid mixture. In fact, the brine with dissolved CO_2 is slightly denser (by almost 1%) than the brine without dissolved CO_2. CO_2 solubility in water increases with increasing pressure and decreases with increasing temperature and water salinity. When CO_2 dissolves in brine, it forms a weak acid.
4. ionic trapping ($H_2CO_3 \leftrightarrow H^+ + HCO^-_3$ and then $HCO_3 \leftrightarrow H^+ + HCO^{2-}_3$) defines the reactions due to ion exchange between the carbonic acid and the formation liquid. It occurs for pH values higher than 6. It is a preliminary step to mineralization if Ca, Fe and Mg cations are available.
5. mineral trapping, involving reactions between the dissolved CO_2 and the formation rock minerals with the geochemical binding to the rock due to mineral precipitation. CO_2-brine-rock interaction enables both mineral dissolution and the generation of secondary minerals. The dissolution and precipitation of formation rocks and caprocks are functions of

their composition, primarily consisting of silicate and aluminosilicate, carbonate, and clay minerals. Silicate minerals work as proton sinks, consuming H^+ and neutralizing the acidity, and hence have more potential for mineral trapping than carbonate minerals. Dissolution of silicate minerals rich in Ca or Mg can release these elements into solution and, if the pH is high enough, can lead to the precipitation of secondary carbonate phases, trapping the CO_2 in secondary minerals. Carbonate dissolution is important because it can dominate the aqueous chemical response by releasing cations such as Ca^{2+}, Mg^{2+}, or Fe^{2+} and buffering pH changes; furthermore, it induces porosity and permeability increase. In terms of rates of dissolution/corrosion, carbonate minerals dissolve/corrode faster than feldspar, plagioclase, and mafic minerals, with quartz being more resistant. Iron and magnesium-rich minerals like olivine are also very reactive. Reaction rates generally increase with temperature and pressure. Thus, the mineral composition of the formation rock, temperature, pressure, salinity and pH of the water are the key parameters that affect the mineral trapping process. In addition, geochemical reactions can affect the integrity of caprocks and wellbores (Jun *et al.*, 2013).

5. Reservoir simulations

The target of the coupled geochemical-fluid flow simulations was to assess which reservoirs would be the best candidates for CO_2 storage based on their capacity and injectivity, but also to investigate the impact of the different trapping mechanisms on CO_2 underground confinement.

Tab. 8 – Production history and Recovery Factors after 30 years.

Model	Number of producers	$Q_{GAS, MAX}$ ($10^3 \cdot m_{SC}^3/d$)	THP_{min} (bar)	Recovery Factor
A	2	500	40	84%
B	2	500	40	64%
C	2	500	40	84%
D	1	100	40	76%
E	4	1000	40	82%
F	2	500	40	71%
G	2	500	40	68%

5.1. Primary production

Each model was initialized in its original conditions, defining the distribution of pressures and saturations throughout the simulation domain.

Before simulating CO_2 injection, all the reservoirs were subject to a production history so that current depletion conditions would be achieved. Thus, a primary production phase was first simulated. For each model, the number of wells (all vertical) and the initial gas rates ($Q_{GAS, MAX}$) were calibrated to obtain a reasonable gas recovery factor after 30 years of production (approximately 85% for reservoirs with a weak aquifer, 70% for reservoirs with a medium aquifer, and 60% for reservoirs with a strong aquifer). The minimum value of the dynamic pressure at the wellhead (THP_{min}) was set at 40 barsa.

The production history and recovery factors are summarized for all models in Table 8.

At the end of the primary production phase, a shut-in period of 15 years was simulated to reproduce the expected conditions of the majority of depleted gas fields, most of which have been abandoned for several years.

5.2. Geochemical interactions

A set of geochemical reactions (Eq. 1 to 17) involving the water and the minerals constituting the reservoir rock was implemented an all the models to describe the interaction of CO_2 with the reservoir (Tab. 9).

The first three reactions represent the dissociation of solubilized CO_2 into bicarbonate and carbonate ions in the aqueous phase, while reactions 4 to 17 describe the dissolution (or precipitation) of minerals. To implement the geochemical reactions within the simulation models, the B-dot model, which is based on the calculation of the chemical activity constant for each component as a function of temperature, was employed. Mineral dissolution or precipitation causes variations in porosity and permeability, which were updated during the simulations using the Kozeny-Carman method.

5.3. CO_2 Injection

The simulation of CO_2 injection into the depleted reservoirs was implemented for each model using the same wells already defined for gas production. Each injector was assigned two constraints: the maximum bottomhole pressure, corresponding to the original pressure of the reservoir; and a maximum Δp at the bottomhole, corresponding to 15% of the initial pressure of the reservoir. Initially, when the reservoir is depleted, the injection rates are limited by the maximum Δp that can be sustained at the well; afterward, when

Tab. 9 – Set of geochemical reactions involving the water and the minerals.

$OH^- + H^+ \leftrightarrow H_2O$	(1)
$CO_2 + H_2O \leftrightarrow H^+ + HCO_3^-$	(2)
$CO_3^{2-} + H^+ \leftrightarrow HCO_3^-$	(3)
$AlNaO_8Si_3$ [*albite*] + $4H^+ \leftrightarrow Al^{3+} + H_2O + Na^+ + 3SiO_2$	(4)
$CaAl_2(SiO_4)_2$ [*anorthite*] + $8H^+ \leftrightarrow 2Al^{3+} + 4H_2O + Ca^{2+} + 2SiO_2$	(5)
$CaCO_3(SiO_4)_2$ [*aragonite*] + $H^+ \leftrightarrow Ca^{2+} + HCO_3^-$	(6)
$CaCO_3$ [*calcite*] + $H^+ \leftrightarrow Ca^{2+} + HCO_3^-$	(7)
$Fe_2Al_2SiO_5(OH)_4$ [*chamosite*, *clorite*] + $10H^+ \leftrightarrow 2Al^{3+} + 2Fe^{2+} + 7H_2O + SiO_2$	(8)
$Mg_5Al_2Si_3O_{10}(OH)_8$ [*clinoclore*, *clorite*] + $16H^+ \leftrightarrow 2Al^{3+} + 5Mg^{2+} + 12H_2O + 3SiO_2$	(9)
$CaMg(CO_3)_2$ [*dolomite*] + $2H^+ \leftrightarrow Ca^{2+} + 2HCO_3^- + Mg^{2+}$	(10)
NaCl [*halite*] $\leftrightarrow Na^+ + Cl^-$	(11)
$K_{0.6}Mg_{0.25}Al_{2.3}Si_{3.5}O_{10}(OH)_2$ [*illite*] + $8H^+ \leftrightarrow 2.3Al^{3+} + 5H_2O + 0.6K^+ + 0.25Mg^{2+} + 3.5SiO_2$	(12)
$KAlSi_3O_8$ [*K-feldspar*] + $4H_+ \leftrightarrow Al^{3+} + 2H_2O + K^+ + 3SiO_2$	(13)
$Al_2Si_2O_5(OH)_4$ [*kaolinite*] + $6H^+ \leftrightarrow 2Al^{3+} + 5H_2O + 2SiO_2$	(14)
$KAl_2(Si_3Al)O_{10}(OH)_2$ [*muscovite*] + $10H^+ \leftrightarrow 3Al^{3+} + K^+ + 6H_2O + 3SiO_2$	(15)
SiO_2 [*quartz*] $\leftrightarrow SiO_{2(aq)}$	(16)
$FeCO_3$ [*siderite*] + $H^+ \leftrightarrow Fe^{2+} + HCO_3^-$	(17)

the pressure in the reservoir increases due to injection, the flow rates are progressively reduced so that the bottomhole pressure does not exceed the initial formation pressure (Tab. 10). The injection stops when the initial formation pressure is reached; duration-wise, all the simulations lasted at least 30 years, while most lasted much longer – up to 160 years.

Each simulation returns the flow rate profile over time at each well, so the injectivity and the mass of CO_2 that can be permanently stored can be determined.

To compare the performance of the different reservoirs, the mass of CO_2 stored after 30 years of injection and the mass of CO_2 stored at the end of the injection (i.e., when the reservoir pressure reached the original value) were considered for each scenario. Furthermore, the authors introduced a parameter named "CO_2 storage efficiency", ε_{CS}, defined as:

$$\varepsilon_{CS} = \frac{M_{CO2}{}^{30\,years}}{M_{CO2}{}^{MAX}} \cdot 100 \quad (18)$$

where $M_{CO2}{}^{30\,years}$ is the mass of CO_2 that can be stored in the first 30 years of injection and $M_{CO2}{}^{MAX}$ is the maximum mass of CO_2 that can be stored in the long term until the initial reservoir pressure is reached.

The reference time of 30 years is arbitrary, yet it was deemed representative of the expected operational life of a CO_2 storage, when significant CO_2 rates can be injected and there is likely a minor need for infrastructure maintenance.

The mass of CO_2 stored after 30 years of injection offers an indirect evaluation of injectivity. In fact, injectivity is the ratio between the injection rate and the associated bottom hole Δp (pressure increase induced at the well by injection). Thus, the higher the injectivity, the larger the volume (hence the mass) of CO_2 that can be stored in the same reference period.

The total mass of CO_2 stored at the end of the injection corresponds to the total storage capacity of the reservoir. However, the time required to fill such capacity, which depends on well injectivity, is also essential to assess the expected performance of a potential storage. The "CO_2 storage efficiency", ε_{CS}, accounts for both capacity and injectivity, thus it is a parameter that provides an overall storage evaluation, and by which different scenarios can be effectively compared.

Tab. 10 – CO_2 injection: number of wells, injection rates and pressure constraint.

Simulation	Reservoir Model	Number of injectors	$Q_{INJ,\,TARGET}$ ($10^3 \cdot m_{SC}{}^3/d$)	$Q_{INJ,min}$ ($10^3 \cdot m_{SC}{}^3/d$)	BHP_{MAX} (bar)
A0	A	2	400	40	207.8
B0	B	2	300	40	103.9
C0	C	2	400	40	311.7
D0	D	1	150	10	207.8
E0	E	4	800	60	207.8
F0	F	2	300	40	207.8
G0	G	2	300	40	207.8

6. Discussion of results

The simulation results about the mass of CO_2 that can be injected into the reservoir and the storage efficiency are reported in Table 11 for all the investigated scenarios.

The mass of CO_2 that can be

Tab. 11 – Simulation results: CO_2 storage capacity and efficiency.

Simulation	$M_{CO2,\ 30\ years}$ (10^6 · tonne)	$M_{CO2,\ MAX}$ (10^6 · tonne)	ε_{CO2}
A0	8.2	15.8	52%
B0	6.1	18.2	34%
C0	8.2	16.6	49%
D0	3.0	3.0	100%
E0	16.4	29.1	56%
F0	6.2	13.1	47%
G0	3.6	12.2	27%

stored during the first 30 years of simulation mainly depends on the pressure constraints assigned to the wells. Conversely, the total (maximum) mass of CO_2 that can be stored in the long term depends on the characteristics of the analyzed reservoir.

It would be expected that the higher the reservoir depth (and thus the pressure), the higher the storage capacity. However, the results tell a different story. Given that models A, B and C share the same GOIP ($5\ 10^9 \cdot sm^3$) and the same aquifer characteristics (r_{aq}/r_{res} = 1.5), it can be inferred that the storage capacity depends on a complex interplay among the reservoir pressure and temperature conditions, the CH_4 and CO_2 compressibility (which decreases with depth, as it can be seen from the values reported in Table 12), and the trapping mechanisms acting on the stored CO_2 (Fig. 3).

In particular, in the case of scenario C0, which represents the deepest reservoir, the pressure and temperature conditions enhance the geochemical reactivity, favoring the precipitation of carbonate minerals. This phenomenon gradually reduces the amount of CO_2 dissolved into the brine, which is then replaced by part of the free CO_2. In turn, the dissolution of CO_2 causes a pressure reduction in the reservoir, allowing the injection of additional CO_2.

If the aquifer characteristics are the same, the size of the reservoir (given by the GOIP) directly affects the maximum mass of CO_2 that can be stored. This can be observed from the results obtained for scenarios A0, D0 and E0. The storage efficiency too is affected by the size of the reservoir because the smaller the volume available for CO_2, the shorter the duration of the injection time (in the case D0, the initial reservoir pressure is reached within 30 years, and so the maximum mass of stored CO_2). Furthermore, a slight increase in CO_2 residual trapping at the expense of the structural trapping can be observed with increasing reservoir volume. This is explained by the larger volume of CO_2 partially penetrating the aquifer and then being trapped by the advancing water front.

Tab. 12 – CH_4 and CO_2 compressibility.

Simulation	Depth (m)	Pressure (bar)	Temperature (°C)	C_{CO2} (1/bar)	C_{CH4} (1/bar)
B0	1000	103.9	32.5	4.04e-2	1.11e-2
A0	2000	207.8	64.9	1.05e-2	5.29e-3
C0	3000	311.7	97.4	4.94e-3	3.08e-3

As expected, the larger the aquifer, the less the mass of CO_2 that can be stored. This is evident from the results obtained for scenarios A0, F0 and G0. The reasons are that encroachment of the aquifer both reduces the porous volume still occupied by free gas (thus limiting the CO_2 that can be structurally trapped) and supports the reservoir pressure. Therefore, CO_2 injection is limited by the pressure rapidly reaching the maximum value allowed. Compared to the reference base case (where the reservoir is confined by a weak aquifer), the presence of a medium to strong aquifer is also responsible for a larger amount of CO_2 trapped by the advancing water (residual trapping) in the short term and by geochemical reactions (solubility, ionic and mineral trapping) in the long term.

Figure 3 summarizes the contribution of the different trapping mechanisms to CO_2 sequestration in the reservoirs after 30 years and 200 years of simulation for all simulated scenarios. The key sensitivity parameters are highlighted in bold for comparison purposes.

7. Conclusions

A set of scenarios representative of Italian depleted gas fields was simulated with 3D coupled geochemical-dynamic numerical models to identify the most adequate characteristics for CO_2 geological storage. The impact of the reservoir depth (thus, pressure and temperature conditions) and volume (expressed by the GOIP but accounting for gas production), and the extension of the confining aquifer, as well as the CO_2 trapping mechanisms, were investigated.

The existence of safety conditions was not examined, as it is considered a prerequisite in the selection of potential storage sites.

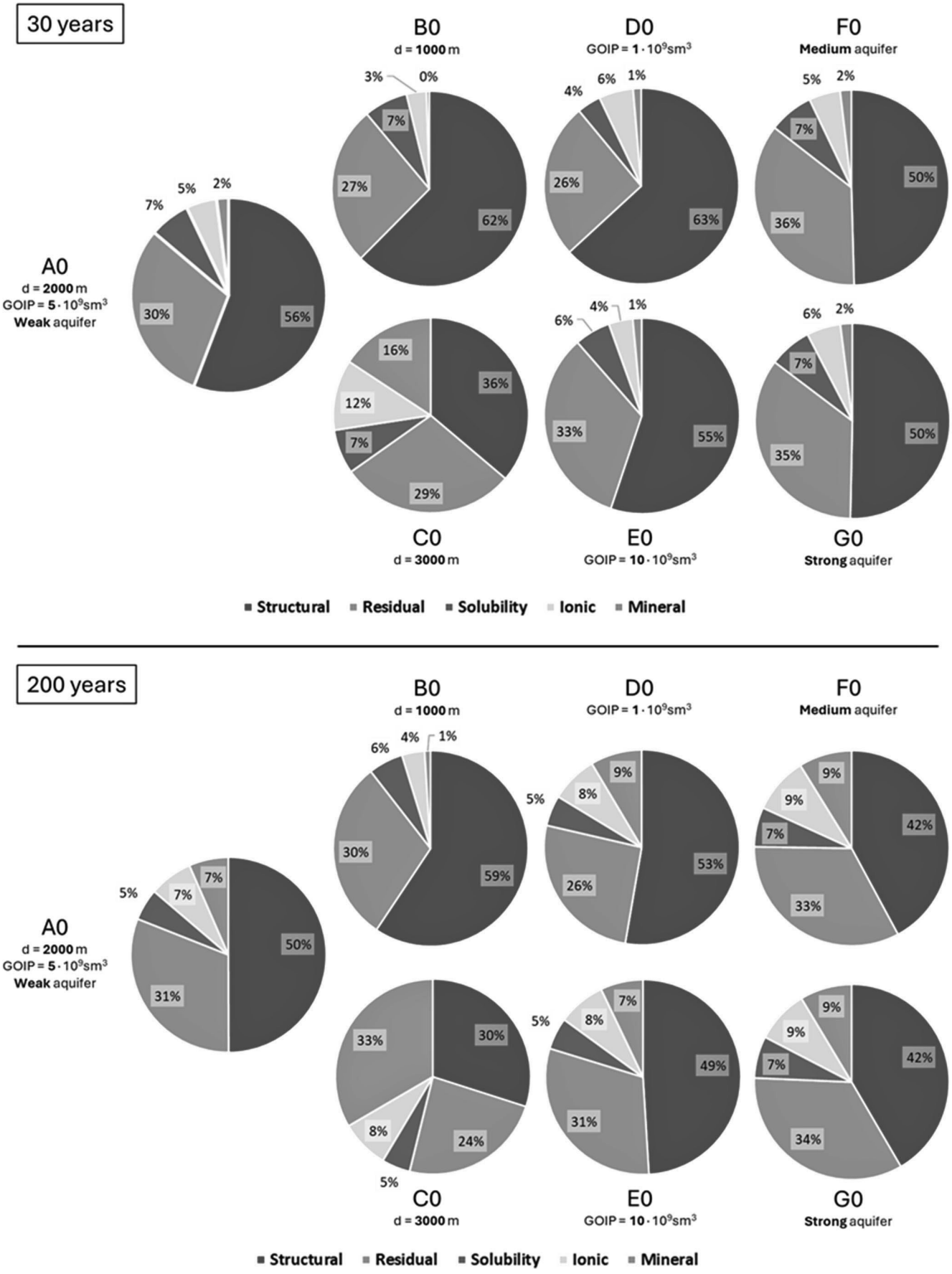

Fig. 3 – Contribution of the different mechanisms to CO_2 trapping in the reservoirs after 30 years and 200 years of simulation. Case A0 is the reference scenario: the key parameters modified for the sensitivities B0, C0, D0, E0, F0, and G0 are highlighted.

Furthermore, the caprock ability to confine CO_2 underground needs to be assessed by laboratory experiments, while geomechanical analyses require including in the model the description of the rock stress-strain behavior and any discontinuity or fault. These aspects were beyond the scope of the work; furthermore, they have been investigated elsewhere (Baldan *et al.*, 2024).

The key findings of the study are provided in the following:

- In general, the Italian depleted gas reservoirs located in the offshore Adriatic area appear to be well suited to CO_2 geological storage. Preliminary assessments are far from being exhaustive, and detailed investigations are needed to assess the system properties, verify the fulfillment of safety requirements, and to reliably forecast the storage performance for real reservoirs. However, the premises are positive.
- The investigated reservoir depth ranges between 1000 and 3000 m. Results show that injectivity slightly decreases with depth, but the storage capacity increases. This is mainly due to the geochemical reactivity of the CO_2, which is enhanced by high temperature and pressure conditions, leading to the precipitation of carbonate minerals and thus allowing more CO_2 to be injected. Therefore, it appears that a depth range of 2000 to 3000 m would be the best option for CO_2 geological storage.
- The reservoir size directly affects the performance of the CO_2 storage. Obviously, the bigger the reservoir, the larger the amount of CO_2 that can be stored and the higher the injectivity, provided that the injectors are located in such a way that interference effects are minimized.
- As expected, the dimension of the aquifer confining the reservoir strongly affects the storage performance. The larger the aquifer, the smaller the injectivity and CO_2 storage capacity (which is initially due to structural trapping), but the larger the amount of CO_2 that is permanently blocked underground by residual and geochemical trapping mechanisms.

The results also highlighted the importance of coupling the geochemical and the fluid flow simulation of CO_2 geological storage. Although the rock mineral composition and the formation water Ph and chemical composition used in this work were not site-specific, it is evident how the storage capacity and the long-term fate of the CO_2 injected underground is determined by the complex interplay among the reservoir pressure and temperature conditions, the CO_2 properties, the reservoir characteristic and the trapping mechanisms.

References

Afagwu, C.C., & Weijermars, R. (2024). *Sensitivity Analysis of Co_2-Migration Paths in Geological Carbon-Dioxide Sequestration: Case Study of the Gorgon Gcs Project*. SSRN. https://doi.org/10.2139/ssrn.4985775

Baldan, S., Ferronato, M., Franceschini, A., Janna, C., Zoccarato, C., Frigo, M., Isotton, G., Collettini, C., Deangeli, C., Rocca, V., Verga, F., Teatini, P. (2024). Unexpected fault activation in underground gas storage. Part II: Definition of safe operational bandwidths. ArXiv Mathematics (online), pp. 31, https://doi.org/10.48550/arXiv.2408.01049

Benetatos, C., Bocchini, S., Carpignano, A., Chiodoni, A., Cocuzza, M., Deangeli, C., Eid, C., Gerboni, R., Lamberti, A., Marasso, S., Massimiani, A., Menin, B., Moscatello, A., Panini, F., Peter, C., Pirri, F., Quaglio, M., Rocca, V., Rovere, A., ... Viberti, D. (2021). How underground systems can contribute to meet the challenges of energy transition. *GEAM*, *1224*(163), 65-80. https://doi.org/10.19199/2021.163-164.1121-9041.065

Bocchini, S., Castro, C., Cocuzza, M., Ferrero, S., Latini, G., Martis, A., Pirri, F., Scaltrito, L., Rocca, V., Verga, F., & Viberti, D. (2017). The Virtuous CO_2 Circle or the Three Cs: Capture, Cache, and Convert. *Journal of Nanomaterials*, *2017*, 1-14. https://doi.org/10.1155/2017/6594151

Carbon Sequestration Leadership Forum. (2021). *Technology Roadmap*.

Carpignano, A., Gerboni, R., Mezza, A., Pirri, C.F., Sacco, A., Sassone, D., Suriano, A., Uggenti, A.C., Verga, F., & Viberti, D. (2023). Italian Offshore Platform and Depleted Reservoir Conversion in the Energy Transition Perspective. *Journal of Marine Science and Engineering*, *11*(8), 1544. https://doi.org/10.3390/jmse11081544

Celia, M.A., Bachu, S., Nordbotten, J.M., & Bandilla, K.W. (2015). Status of CO_2 storage in deep saline aquifers with emphasis on modeling approaches and practical simulations: Status of CO_2 storage in deep saline aquifer. *Water Resources Research*, *51*(9), 6846-6892. https://doi.org/10.1002/2015WR017609

Chadwick, R.A., & British Geological Survey (A c. Di). (2008). *Best practice for the storage of CO_2 in saline aquifers: Observations and guidelines from the SACS and CO2STORE projects*. British Geological Survey.

European Commission, & Joint Research Centre. (2024). *GHG Emissions of all world countries* (pp. 283-283). Publications Office of the European Union. https://data.europa.eu/doi/10.2760/4002897

Furre, A.-K., Eiken, O., Alnes, H., Vevatne, J.N., & Kiær, A.F. (2017). 20 Years of Monitoring CO_2-injection at Sleipner. *Energy Procedia*, *114*, 3916-3926. https://doi.org/10.1016/j.egypro.2017.03.1523

Hansen, O., Gilding, D., Nazarian, B., Osdal, B., Ringrose, P., Kristoffersen, J.-B., Eiken, O., & Hansen, H. (2013). Snøhvit: The History of Injecting and Storing 1 Mt CO_2 in the Fluvial Tubåen Fm. *Energy Procedia*, *37*,

3565-3573. https://doi.org/10.1016/j.egypro.2013.06.249

Jun, Y.-S., Giammar, D.E., & Werth, C.J. (2013). Impacts of Geochemical Reactions on Geologic Carbon Sequestration. *Environmental Science & Technology*, *47*(1), 3-8. https://doi.org/10.1021/es3027133

Ma, J., Li, L., Wang, H., Du, Y., Ma, J., Zhang, X., & Wang, Z. (2022). Carbon Capture and Storage: History and the Road Ahead. *Engineering*, *14*, 33-43. https://doi.org/10.1016/j.eng.2021.11.024

Northern Lights. (s.d.). Recuperato 19 dicembre 2024, da https://www.equinor.com/energy/northern-lights

Peng, D.-Y., & Robinson, D.B. (1976). A New Two-Constant Equation of State. *Industrial & Engineering Chemistry Fundamentals*, *15*(1), 59-64. https://doi.org/10.1021/i160057a011

Ringrose, P.S., Mathieson, A.S., Wright, I.W., Selama, F., Hansen, O., Bissell, R., Saoula, N., & Midgley, J. (2013). The In Salah CO_2 Storage Project: Lessons Learned and Knowledge Transfer. *Energy Procedia*, *37*, 6226-6236. https://doi.org/10.1016/j.egypro.2013.06.551

Rocca, V., & Viberti, D. (2013). Environmental sustainability of oil industry. *American Journal of Environmental Sciences*, *9*(3), 210-217. https://doi.org/10.3844/ajessp.2013.210.217

Shi, J.-Q., Imrie, C., Sinayuc, C., Durucan, S., Korre, A., & Eiken, O. (2013). Snøhvit CO_2 Storage Project: Assessment of CO_2 Injection Performance Through History Matching of the Injection Well Pressure Over a 32-months Period. *Energy Procedia*, *37*, 3267-3274. https://doi.org/10.1016/j.egypro.2013.06.214

Spagnoli, F., Dinelli, E., Giordano, P., Marcaccio, M., Zaffagnini, F., & Frascari, F. (2014). Sedimentological, biogeochemical and mineralogical facies of Northern and Central Western Adriatic Sea. *Journal of Marine Systems*, *139*, 183-203. https://doi.org/10.1016/j.jmarsys.2014.05.021

Suriano, A., Peter, C., Benetatos, C., & Verga, F. (2022). Gridding Effects on CO_2 Trapping in Deep Saline Aquifers. *Sustainability*, *14*(22), 15049. https://doi.org/10.3390/su142215049

Tanase, D., Saito, H., Honda, T., Mori, A., Wada, Y., Higuchi, K., & Tanaka, J. (2021, marzo). *Progress of CO_2 injection and monitoring of the Tomakomai CCS Demonstration Project*. 15th International Conference on greenhouse Gas Control Technologies, GHGT-15, Abu Dhabi, UAE.

Trupp, M., Ryan, S., Barranco Mendoza, I., Leon, D., & Scoby-Smith, L. (2021). Developing the world's largest CO_2 Injection System – a history of the Gorgon Carbon Dioxide Injection System. *SSRN Electronic Journal*. https://doi.org/10.2139/ssrn.3815492

Verga, F. (2018). What's Conventional and What's Special in a Reservoir Study for Underground Gas Storage. *Energies*, *11*(5), 1245. https://doi.org/10.3390/en11051245

ViDEPI. access at https://www.videpi.com/videpi/videpi.asp

Working Group III of the Intergovernmental Panel on Climate Change. (2005). *IPCC Special Report on Carbon Dioxide Capture and Storage*. Cambridge University Press.

Acknowledgements

The authors would like to acknowledge the MASE – Ministry of the Environment and Energy Safety (formerly Ministry of the Ecological Transition) for providing support to the development of this study.